J. Plasma Physics (2012), vol. 78, part 5, pp. 545–551. © Cambridge University Press 2012
doi:10.1017/S0022377812000268

Nonlinear low-frequency structures in an electron–positron–ion plasma

S. MOOLLA[1], I. J. LAZARUS[2] and R. BHARUTHRAM[3]

[1]School of Chemistry and Physics, University of KwaZulu-Natal, Durban, 4000, South Africa
(moollas@ukzn.ac.za)
[2]Department of Mathematics, Statistics and Physics, Durban University of Technology, Durban, 4000, South Africa
[3]Office of the Deputy Vice Chancellor, University of the Western Cape, Modderdam Road, Belville, 7535, South Africa

(Received 7 December 2011; revised 6 February 2012; accepted 8 February 2012; first published online 20 March 2012)

Abstract. Nonlinear ion cyclotron and ion-acoustic waves have been studied in an electron–positron–ion plasma. Using Boltzmann distributions for the electrons and positrons and fluid equations for the ions, a set of nonlinear equations in the rest frame of the propagating wave is derived and numerically solved for the electric field. A scan of parameter space reveals a range of solutions for the parallel electric field, from sinusoidal to sawtooth to highly spiky waveforms. The results are compared with satellite observations.

1. Introduction

There has been a great deal of interest in linear and nonlinear wave phenomena in electron–positron–ion (EPI) plasmas in recent years. Electron–positron plasmas are thought to exist in many astrophysical environments such as the early universe, galactic nuclei and pulsar magnetospheres to name a few. They are believed to be naturally generated by pair production. In addition, most of these astrophysical plasmas contain ions as well, constituting an EPI plasma. In the recent past, the study of nonlinear wave propagation in EPI plasmas has been extended to investigate nonlinear structures similar to the broadband electrostatic noise (BEN) observed in the Earth's magnetosphere. Over the past 30 years, satellite observations have confirmed the presence of BEN in different regions of the Earth's magnetosphere, including the polar cusp region [1] and along auroral field lines [2]. Observations by Geotail [3], POLAR [4] and FAST [5] spacecrafts have confirmed the presence of nonlinear structures in BEN. In particular, these observations have shown that the nonlinear, time domain structures associated with the electric field parallel to the ambient magnetic field exhibit spiky wave forms. Reddy *et al.* [6] have used a novel fluid theory approach to examine nonlinear low-frequency electric field structures in an electron–ion plasma for which the ions were assumed to be cold. For sufficiently large values of the driver electric field, the governing equation for the electric field, which includes a nonlinear coupling between the ion-acoustic wave and ion cyclotron oscillations, is found to admit both sawtooth and spiky periodic solutions which are in very good agreement with the observations of Ergun *et al.* [5].

Following the approach of Reddy *et al.* [6], Bharuthram *et al.* [7] extended this model to show that finite ion temperature gave rise to wave dispersion and suppressed the nonlinearity in the ion cyclotron wave.

In a later study, Moolla *et al.* [8] studied high-frequency nonlinear waves in the Earth's magnetosphere. They considered a three-component plasma model consisting of hot electrons, cold electrons and cold ions. The transition from sinusoidal to sawtooth to highly spiky waveforms occurred as the amplitude of the driving electric field E_0 was increased. In addition, their results showed that the hot electrons could be accelerated in bursts leading to rapid changes in the periodicity of the nonlinear structures.

Reddy *et al.* [9] studied nonlinear low-frequency electrostatic oscillations in a magnetized plasma consisting of protons, electrons and oxygen ion beams. They went on to show that a range of periodic solutions varying from sinusoidal to sawtooth and highly spiky wave forms. Moolla *et al.* [10] offered an explanation for high-frequency BEN in the Earth's magnetosphere using a three-component magnetized plasma consisting of hot electrons, cool electrons and cool ions. They showed that the ratio of the pulse widths and periods of the Electrostatic Solitary Waves (ESWs) were constant, confirming the experimental observations of Kojima *et al.* [11]. They showed that increasing the cool electron temperature resulted in a broadening of the waves, with an increase of the period and nonlinearity. Moolla *et al.* [12] used a three-component plasma model consisting of Boltzmann protons and electrons and a cold oxygen ion beam to study spiky structures arising from a coupling of two low-frequency modes, namely the oxygen ion cyclotron and the oxygen ion-acoustic mode. Including the charge separation effect, they showed a range of solutions from sinusoidal to sawtooth to highly spiky, depending on parameter selections.

Ghosh and Bharuthram [13] investigated nonlinear propagation characteristics of ion-acoustic waves in an electron–positron–ion–dust plasma. They showed the

https://doi.org/10.1017/S0022377812000268 Published online by Cambridge University Press

system supported both compressive and rarefactive solitons and double layers, depending on parameter regimes. In a later paper, Ghosh and Bharuthram [14] studied the effects of Landau damping on small but finite amplitude ion-acoustic solitary waves in an EPI plasma. Their results showed that the presence of positrons reduced the Landau damping rate.

Abdelsalam *et al.* [15] investigated fully nonlinear propagation of ion-acoustic solitary waves in a collisionless dense/quantum EPI plasma. Their calculations revealed that both subsonic and supersonic ion-acoustic solitary waves may exist for low values of the positron-to-electron number density ratio. Dubinov and Sazonkin [16] presented an analytical nonlinear gasdynamic theory of ion-acoustic waves in an EPI plasma for the case in which all the plasma components in the wave undergo polytropic compression and rarefaction. They found an exact solution to the basic equations and used the Bernoulli pseudopotential method to analyze the solution. They determined parameter ranges in which periodic waves and solitary nonlinear waves (solitons) existed. They further showed that these ranges did not overlap and that the propagation velocity of a solitary wave was always higher than the linear ion-acoustic velocity.

In this paper, we explore the existence of such nonlinear electric field structures in an EPI plasma assuming quasineutrality, thereby focussing on low-frequency fluctuations on the ion time scale. The layout of this paper is as follows. In Sec. 2, we present the basic theory and the numerical results are presented in Sec. 3. Finally, our findings are summarized in Sec. 4.

2. Basic theory

We consider an electron–positron plasma with an ion species drifting along the magnetic field with speed v_0. Wave propagation is taken to be in the x direction at an angle θ to the magnetic field $\vec{B}_0$, which is assumed to be in the $x-z$ plane. We allow spatial variation only in the x direction. On the ion time scale, the density distribution for the electrons and positrons is taken to be Boltzmann, given, respectively, by

$$n_e = n_{e0}\exp(e\phi/T_h), \tag{1}$$

and

$$n_p = n_{p0}\exp(-e\phi/T_h), \tag{2}$$

where $n_{e0,p0}$ and T_h are the ambient densities and temperature of the electrons and positrons, respectively. The basic set of fluid equations for the positive ions is given by

$$\frac{\partial n_i}{\partial t} + \frac{\partial n_i v_{ix}}{\partial x} = 0, \tag{3}$$

$$\frac{\partial v_{ix}}{\partial t} + v_{ix}\frac{\partial v_{ix}}{\partial x} + \frac{1}{n_i m_i}\frac{\partial p_i}{\partial x} = -\frac{e}{m_i}\frac{\partial \phi}{\partial x} + \Omega_i v_{iy}\sin\theta, \tag{4}$$

$$\frac{\partial v_{iy}}{\partial t} + v_{ix}\frac{\partial v_{iy}}{\partial x} = \Omega_i v_{iz}\cos\theta - \Omega_i v_{ix}\sin\theta, \tag{5}$$

$$\frac{\partial v_{iz}}{\partial t} + v_{ix}\frac{\partial v_{iz}}{\partial x} = -\Omega_i v_{iy}\cos\theta, \tag{6}$$

$$\frac{\partial p_i}{\partial t} + v_{ix}\frac{\partial p_i}{\partial x} + 3p_i\frac{\partial v_{ix}}{\partial x} = 0, \tag{7}$$

where n_i is the ion density, v_{ix}, v_{iy} and v_{iz} are the components of the ion velocity along the x, y and z directions, respectively, $\Omega_i = eB_0/m_i$ is the ion cyclotron frequency, m_i is the ion mass, ϕ is the electrostatic potential of the waves and p_i is the ion pressure. For the low-frequency domain, our system is closed with the quasineutrality condition $n_e = n_i + n_p$. For most of our discussion, the ions are stationary. However, we also look at the effect of a drifting ion beam.

2.1. Linear analysis

Before proceeding with the nonlinear analysis, we investigate the linear modes of the system. In this limit, (1)–(7) give rise to the following dispersion relation for stationary ions:

$$\omega^2 = \frac{1}{2}\left(\Omega_i^2 + A^2\right) \pm \frac{1}{2}\left[\left(\Omega_i^2 + A^2\right)^2 - 4A^2\Omega_i^2\cos^2\theta\right]^{1/2}, \tag{8}$$

where $A^2 = 3k^2v_{ti}^2 + (\frac{n_{i0}}{n_{e0}+n_{p0}})k^2C_s^2$, $v_{ti} = \sqrt{\frac{T_i}{m_i}}$ is the ion thermal speed and $C_s = \sqrt{\frac{T_h}{m_i}}$ is the ion-acoustic speed. The solution to this equation yields two roots:

$$\omega_+^2 = \left(\Omega_i^2 + A^2\right) - \frac{A^2\Omega_i^2\cos^2\theta}{\Omega_i^2 + A^2}, \tag{9}$$

and

$$\omega_-^2 = \frac{A^2\Omega_i^2\cos^2\theta}{\Omega_i^2 + A^2}. \tag{10}$$

We identify ω_+ as the higher frequency ion cyclotron mode and ω_- as the lower frequency ion-acoustic mode. For cold ions and in the absence of positrons, these results reduce to those of Reddy *et al.* [6] in which they considered a two-component plasma consisting of protons, electrons and cold ions.

2.2. Nonlinear analysis

For the analysis, we transform to a stationary frame $s = (x - Vt)/(V/\Omega_i)$ and normalize v, t, x and ϕ with respect to the ion-acoustic speed $C_s = (T_h/m_i)^{1/2}$, Ω_i^{-1}, $\rho_i = C_s/\Omega_i$ and T_h/e, respectively.

In (3)–(7), we replace $\frac{\partial}{\partial t}$ by $-\Omega_i\frac{\partial}{\partial s}$ and $\frac{\partial}{\partial x}$ by $(\Omega_i/V)\frac{\partial}{\partial s}$. In addition, we define the normalized electric potential $\psi = e\phi/T_h$ and the electric field $E = -\frac{\partial\psi}{\partial s}$. We use the following (initial) conditions:
$\psi = 0$, $\partial\psi/\partial s = E_0$, $\partial^2\psi/\partial s^2 = 0$, $n_i = n_{i0}$ and $v_x = v_0\cos\theta$ at $s = 0$. The evolution of the plasma is then determined by the following set of nonlinear, normalized (densities with respect to n_{e0} and pressure with respect to $p_0 = n_{e0}T_h$) first order differential equations, where the additional 'n' subscript inserted indicates normalized

https://doi.org/10.1017/S0022377812000268 Published online by Cambridge University Press

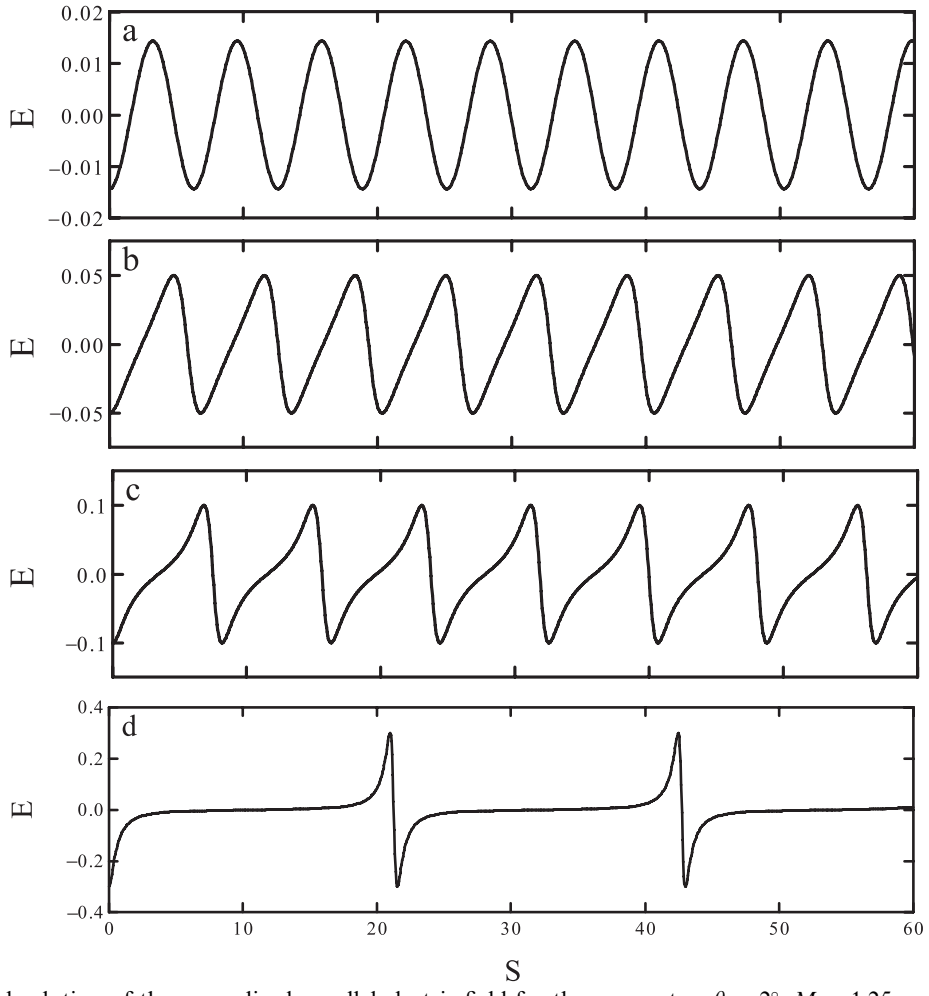


Figure 1. Numerical solution of the normalized parallel electric field for the parameters $\theta = 2^\circ$, $M = 1.25$, $n_{p0}/n_{e0} = 0.5$, $\delta = 0.0$, $T_i/T_h = 0.0$ and $E_0 = 0.015$(a), 0.05(b), 0.10(c) and 0.30(d).

quantities

$$E = \frac{n_{in}^3 M v_{iyn} \sin\theta}{1 + R\frac{n_{p0}}{n_{e0}}\exp(-\psi) + R\exp(\psi)}, \tag{11}$$

$$\frac{\partial n_{in}}{\partial s} = \frac{n_{in}^3[-E - M v_{iyn}\sin\theta]}{R}, \tag{12}$$

$$\frac{\partial p_{in}}{\partial s} = \frac{3p_{in}}{n_{in}}\frac{n_{in}^3[-E - M v_{iyn}\sin\theta]}{R}, \tag{13}$$

$$\frac{\partial v_{iyn}}{\partial s} = n_{in}(M - \delta\cos\theta)^{-1}\Big/\left(\frac{n_{i0}}{n_{e0}}\right),$$

$$\left[M\sin\theta\left(M - \frac{(M - \delta\cos\theta)\frac{n_{i0}}{n_{e0}}}{n_{in}}\right) - M v_{izn}\cos\theta\right], \tag{14}$$

$$\frac{\partial v_{izn}}{\partial s} = n_{in}\frac{M v_{iyn}\cos\theta}{(M - \delta\cos\theta)\frac{n_{i0}}{n_{e0}}}. \tag{15}$$

In (11)–(15), $R = (\frac{n_{i0}}{n_{e0}})^2(M - \delta\cos\theta)^2 - 3n_{in}p_{in}$, where $M = V/C_s$ is the Mach number, n_{i0}/n_{e0} is the normalized equilibrium ion density and $\delta = v_0/C_s$ is the normalized flow velocity of the ion beam at $s = 0$. Note that if δ is positive (negative), it corresponds to parallel (antiparallel) ion drift, i.e. the ion flow can be in the same direction as the wave or in the opposite direction. The normalized electron and positron density distributions are given by

$$n_{en} = \exp(\psi), \tag{16}$$

and

$$n_{pn} = \frac{n_{p0}}{n_{e0}}\exp(-\psi), \tag{17}$$

where n_{p0}/n_{e0} is the normalized positron ambient density.

3. Numerical results

Equations (11)–(17) are solved using the Runge–Kutta technique [17] for plasma parameters encountered on the auroral field lines. The method involves providing initial values to plasma parameters and using the RK-4 subroutine [17] to advance the functions with a suitable step length. The initial conditions have been calculated self consistently. The results are discussed next.

https://doi.org/10.1017/S0022377812000268 Published online by Cambridge University Press

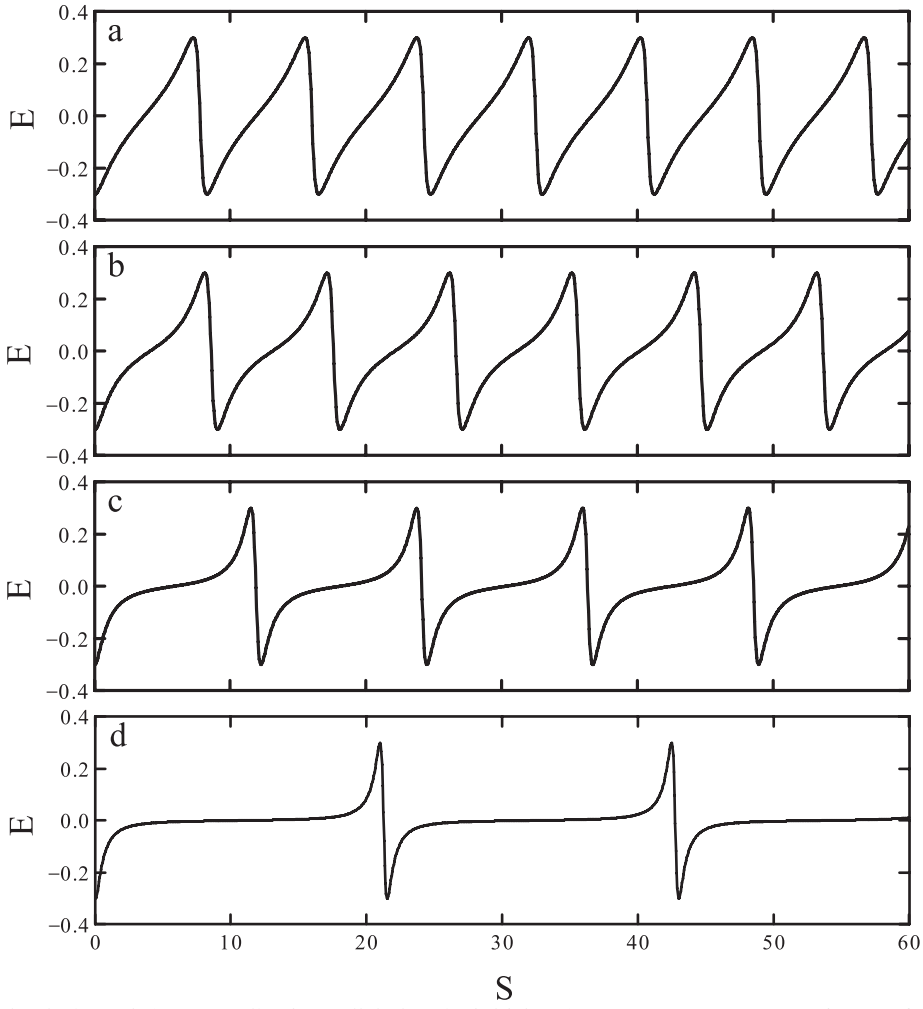


Figure 2. Numerical solution of the normalized parallel electric field for the parameters $E_0 = 0.3$, $\theta = 2°$, $\delta = 0.0$, $T_i/T_h = 0.0$, $M = 1.25$ and $n_{p0}/n_{e0} = 0.0$(a), 0.1(b), 0.3(c) and 0.5(d).

3.1. *Effect of the amplitude, E_0, of the driving electric field*

It is noted upfront that in the absence of positrons ($n_{p0} = 0$), our model reduces to that of Bharuthram *et al.* [7] and we reproduce their results for identical parameters. For our model, in Figs. 1(a)–(d) for a fixed Mach number of $M = 1.25$, we vary the driver strength, E_0. In these figures, the fixed parameters are $\theta = 2°$, $\delta = 0.0$ (i.e. the ions are stationary for the initial studies), n_{p0}/n_{e0} =0.5 and $\alpha = T_i/T_h$ =0.0. For small values of E_0 (0.015), the parallel electric field shows sinusoidal behavior with a period of $\approx 1.0\tau_{ci}$ where $\tau_{ci} = 2\pi/\Omega_i$ is the ion cyclotron period. We thus identify this as being the ion cyclotron mode. As E_0 increases, we have a transition to the ion-acoustic mode with increasing nonlinearity which results in a highly spiky electric field (Fig. 1(d)), with a period of $\approx 3.5\tau_{ci}$. It is found that the introduction of positrons has reduced the strength of the initial driving electric field required for the onset of the spiky structures. In the work of Bharuthram *et al.* [7], the onset of spikes occurred with an initial driving electric field of 1.1 while for the same fixed parameters, the addition of positrons has reduced the initial driving field to 0.3 for the onset of spikes. Hence, the positrons have the effect of promoting wave steepening and enhancing nonlinearity. The value of these periods is consistent with the measurements for $E_\parallel$ (the magnetic field-aligned electric field component) observed by the FAST satellite in Fig. 6 of Ergun *et al.* [5], where the time series of the parallel electric field revealed a spiky wave form at a lower frequency compared to the perpendicular electric field.

3.2. *Effect of the equilibrium positron density*

The effect on the parallel electric field structures due to a variation in the equilibrium positron density is shown in Figs. 2(a)–(d). For small values of $\frac{n_{p0}}{n_{e0}}$ (0.0 and 0.1), the electric field structures are sawtooth in nature with periods of about $1.3\tau_{ci}$. As $\frac{n_{p0}}{n_{e0}}$ increases to 0.5, the waveform becomes highly spiky with a period of about $3.3\tau_{ci}$. Hence, increasing the density of the positrons enhances the nonlinearity and the spiky structures are easier to generate.

https://doi.org/10.1017/S0022377812000268 Published online by Cambridge University Press

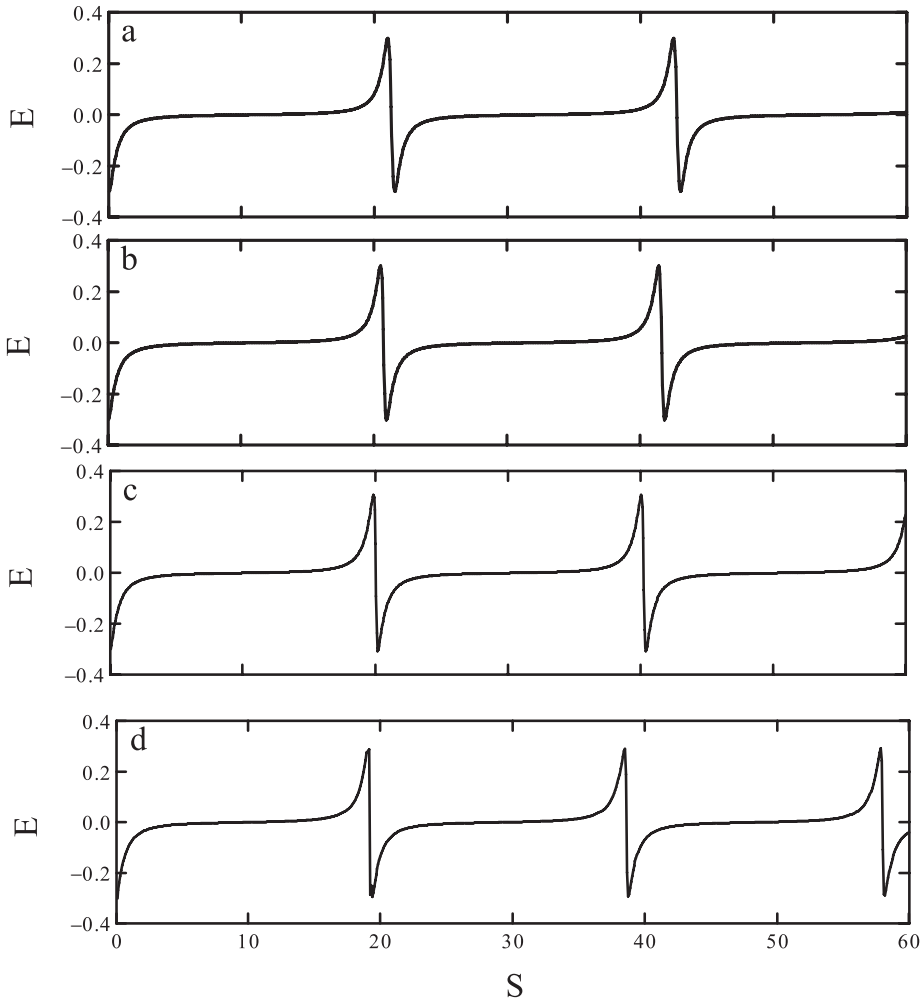


Figure 3. Numerical solution of the normalized parallel electric field for the parameters $E_0 = 0.3$, $M = 1.25$, $\theta = 2°$, $n_{p0}/n_{e0} = 0.5$, $\delta = 0.0$ and $T_i/T_h = 0.0$(a), 0.05(b), 0.1(c) and 0.15(d).

3.3. *Effect of ion temperature*

Figure 3 illustrates the effect of the ion–electron temperature ratio, T_i/T_h on the parallel field. For other parameters fixed as in Fig. 2, T_i/T_h is increased from 0.0 (Fig. 3(a)) to 0.15 (Fig. 3(d)). An increase in this ratio results in waveforms with increasing frequency, with no effect on the nonlinearity of the waves. The period of the waves decreases from $3.4\tau_{ci}$ to $3.0\tau_{ci}$. This behavior can be seen from (10) which can be rewritten as

$$\omega_-^2 = \frac{\Omega_i^2 \cos^2\theta}{\frac{\Omega_i^2}{A^2} + 1}, \tag{18}$$

where as A increases, ω_- also increases resulting in a decrease in the period of the waves. This behavior is consistent with those of Bharuthram *et al.* [7]. In their studies, however, the nonlinearity of the waves was suppressed with increasing the ion temperature which is due to enhanced dispersive effects. Hence, we can conclude that the addition of positrons promotes wave steepening.

3.4. *Effect of the ion drift*

Finally, we investigate the effect of the ion drift velocity on the electric field, as seen in Figs. 4(a)–(e), with other parameters the same as in Fig. 2. From these figures, it is seen that ion flow antiparallel to $\vec{B}_0$ (δ negative) results in higher period waves and as the flow becomes parallel to $\vec{B}_0$ (δ positive) the period decreases. All the structures were found to be of the spiky type for the selected parameters. The period of the waves varies from $4.8\tau_{ci}$ for $\delta = -0.2$ to $2.3\tau_{ci}$ for $\delta = +0.2$, and can be interpreted as the ion-acoustic mode. The behavior of the period with the ion drift is the same as that found by Moolla *et al.* [8] for the high-frequency studies. The behavior of the electric field structures follows a similar pattern to that of Reddy *et al.* [9]. It is seen that the period of the spiky structures varies with the ion drift velocity. Noting that the satellite observations show that the period of the spiky structures varies rapidly [11], one may infer that this could be due to the drifting particles being accelerated in bursts [8].

https://doi.org/10.1017/S0022377812000268 Published online by Cambridge University Press

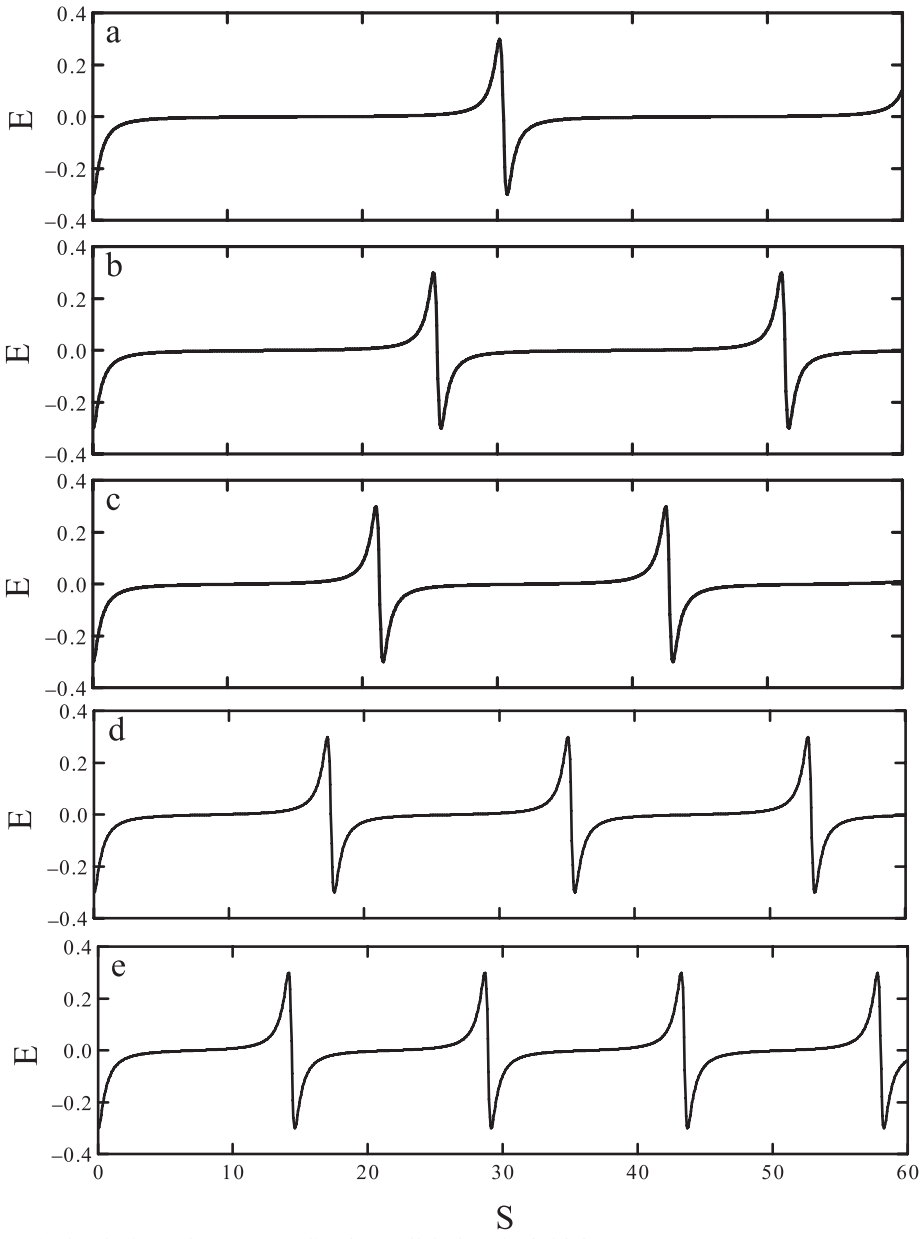


Figure 4. Numerical solution of the normalized parallel electric field for the parameters $E_0 = 0.3$, $M = 1.25$, $\theta = 2^\circ$, $n_{p0}/n_{e0} = 0.5$, $T_i/T_h = 0.0$ and $\delta = -0.2$(a), -0.1(b), 0.0(c), 0.1(d) and 0.2(e).

4. Conclusion

In this paper, we have used an EPI plasma to investigate nonlinear, low-frequency waves arising from a coupling of two low-frequency modes, namely, the ion cyclotron and the ion-acoustic mode. The presence of a positron component is found to have a significant impact on the nonlinear structures. The driving electric field E_0 needed to excite the nonlinear structures is much lower in the presence of positrons, with a transition from an ion cyclotron to ion-acoustic mode with increasing E_0 as the nonlinear structures evolve from a sinusoidal, through a sawtooth, to a spiky waveform. We have found that larger initial driving amplitudes result in more spiky structures with a reduction in the wave frequency. We identify these as the spiky ion-acoustic mode. The positron density also played a crucial role in evolution of the electric field structures. The spiky structures associated with the driven ion-acoustic mode only existed for high equilibrium positron density, with smaller densities giving rise to the ion cyclotron oscillations. In addition, the drift velocity of the ions were shown to have a significant impact on the waves, with antiparallel (parallel) ion flow resulting in lower (higher) frequency waves, with no effect on the amplitude of the nonlinear structures. Finally, the ion temperature was also found to affect the periods of the spiky electric

https://doi.org/10.1017/S0022377812000268 Published online by Cambridge University Press

field, with an increase in the ion temperature resulting in higher frequency waves. For our model, the unnormalized electric field is given as

$$E_{UN} = -\frac{\partial \phi}{\partial x} = \frac{\Omega_i}{V}\frac{\partial \phi}{\partial s} = \frac{\Omega_i}{MC_s}T_h/e\frac{\partial \psi}{\partial s} = \frac{E}{M}\frac{T_h}{e\rho_i}. \quad (19)$$

For the spiky structures obtained in this paper, for T_h varying from 10 eV to 100 eV and for a magnetic field of about 13000 nT, (19) predicts amplitudes in the range from about 200 mV/m to 800 mV/m. The amplitude of the parallel electric field observed by the FAST satellite [5] is about 700 mV/m, which is within the predicted range of values, noting that the observations were in a pure electron–ion plasma. Our particular results could be applicable in understanding the nonlinear structures observed in EPI plasmas existing in pulsar magnetospheres [18] and active galactic nuclei [19].

References

[1] Gurnett, D. A. and Frank, L. A. 1978 *J. Geophys. Res.* **83**, 1447.

[2] Gurnett, D. A. and Frank, L. A. 1977 *J. Geophys. Res.* **82**, 1031.

[3] Matsumoto, H., Kojima, H., Miyatake, T., Omura, Y., Okada, M. and Tsutsui, M. 1994 *Geophys. Res. Lett.* **21**, 2915.

[4] Mozer, F. S., Ergun, R. E., Temerin, M., Cattell, C., Dombeck, J. and Wygant, J. 1997 *Phys. Rev. Lett.* **79**, 1281.

[5] Ergun, R. E., Carlson, C. W., McFadden, J. P., Mozer, F. S., Delroy, G. T., Peria, W., Chaston, C. C., Temerin, M., Elphic, R., Strangeway, R., *et al.* 1998 *Geophys. Res. Lett.* **25**, 2025.

[6] Reddy, R. V., Lakhina, G. S., Singh, N. and Bharuthram, R. 2002 *Nonlinear Proc. Geophys.* **9**, 25.

[7] Bharuthram, R., Reddy, R. V., Lakhina, G. S. and Singh, N. 2002 *Physica Scripta* **T98**, 137.

[8] Moolla, S., Bharuthram, R., Singh, S. and Lakhina, G. S. 2003 *PRAMANA - J. Phys.* **61**, 1.

[9] Reddy, R. V., Singh, S. V., Lakhina, G. S. and Bharuthram, R. 2006 *Earth Planets Space* **58**, 1227.

[10] Moolla, S., Bharuthram, R., Singh, S., Lakhina, G. S. and Reddy, R. V. 2007 *J. Geophys. Res.* **112**, A07214.

[11] Kojima, H., Matsumoto, H., Miyatake, T., Nagano, I., Fujita, A., Frank, L. A., Mukai, T., Paterson, W. R., Saito, Y. and Machida, S. 1994 *Geophys. Res. Lett.* **21**, 2919.

[12] Moolla, S., Bharuthram, R., Singh, S., Lakhina, G. S. and Reddy, R. V. 2010 *Phys. Plasmas* **17**, 1.

[13] Ghosh, S. and Bharuthram, R. 2008 *Astrophys. Space Sci.* **314**, 121.

[14] Ghosh, S. and Bharuthram, R. 2011 *Astrophys. Space Sci.* **331**, 163.

[15] Abdelsalam, U. M., Moslem, W. M. and Shukla, P. K. 2008 *Phys. Lett.* A **372**, 4057.

[16] Dubinov, A. E. and Sazonkin, M. A. 2009 *Plasma Phys. Rep.* **35**, 14.

[17] Press, W. H., Teukolsky, S. A., Vetterling, W. T. and Flannery, B. P. 1996 *NUMERICAL RECIPES in Fortran 90 - The Art of Parallel Scientific Computing.* Vol. 2. New York: Cambridge University Press.

[18] Michel, F. C. 1982 *Rev. Mod. Phys.* **54**, 1.

[19] Miller, H. R. and Witta, P. J. 1987 *Active Galactic Nuclei.* Berlin: Springer, p. 202.

https://doi.org/10.1017/S0022377812000268 Published online by Cambridge University Press